31st Congress of the International Council of the Aeronautical Sciences

Belo Horizonte, Brazil; September 09-14, 2018

PASSIVE CONTROL METHOD IN ATTENUATING SELF-INDUCED ROLL OSCILLATIONS OF LOW-ASPECT-RATIO WINGS USING OBLIQUE SLOT BLEED

HOU Tuo*, CHENG Changfu*, HU Tianxiang*
***LuShijia Laboratory, Beihang University**

Keywords: *MAV, Low aspect ratio wings, Self-induced oscillations, Wing tip slot*

Abstract

The purpose of this paper is to introduce an effective near tip slot configuration for low-aspect-ratio rectangular wings, to attenuate its self-induced roll oscillations at large angle of attack. A series wind tunnel tests were conducted on 9 different test models, each with a narrow near tip slot (3mm) orientated differently, at the wind speed of 10m/s, with the angle of attack ranging from 0° to 30°. Among all the models tested, the model with slot orientation angle of $\beta = 45°$ have demonstrated the best effect on attenuating the oscillation. At $\alpha = 26°$, the RMS roll angles was suppressed by $\Delta\Phi_{rms,max} = 47°$. The effect to lessen roll frequency has also been observed. For other tested models, the $\beta = 30°$ model and the $\beta = 120°$ model have also shown attenuation effect in general. PIV measurements showed that the bleed results from wing tip slot may have affected the generation and reattachment of wing tip vortex, and thus result in attenuation or enhancement of self-induced roll oscillations.

1 General Introduction

1.1 Self-Induced Roll Oscillation

Micro Air Vehicles (MAV) are receiving increasing interests due to its unique advantages and broad applications. While during MAV tests, an unwanted large-amplitude roll oscillation phenomenon occurred at large angle of attack, also known as wing rock. This could lead to serious consequences during MAV flight. This paper introduced a passive flow control method using slot near wing tip to attenuate this phenomenon regarding a common low-aspect-ratio rectangular wing configuration.

1.2 Previous Study

Previous studies regarding this matter mainly focused on slender delta wings and slender rectangular wings[1, 2, 3]. Due to MAV's small size and low speed, most MAVs are operating in a low Reynolds number condition ($Re \approx 3 \times 10^4 \sim 3 \times 10^5$), thus previous findings shall not apply to MAV designing. According to a study by Bakaul et al.[4], in such condition, especially with large AoA, low-aspect-ratio wings can generate extra lift due to its 3D flow structure. Thus LAR wings are ideal choice for MAVs. For passive methods regarding LAR rectangular wings, Hu et al.[5, 6] recently found that by adding slot near wing tip, wing rock can be attenuated effectively. With certain configurations, roll oscillation can be completely suppressed.

2 Methodology

2.1 Closed Loop Wind Tunnel

The experiment was conducted at D1 wind tunnel at Beihang University, a closed loop open test section wind tunnel with a nozzle of $1.02m \times 0.76m$ and a collector of $1.07m \times 0.82m$. The length of the test section is $1.45m$, and the tur-

bulence level of this wind tunnel is less than 3%.

2.2 Free-to-Roll Device

The free-to-roll device used in this experiment was consisted of a shaft held by two concentric bearings. The shaft was connect to a potentiometer to record the roll movement of the shaft. The data acquisition device was NATIONAL INSTRUMENTS USB-6210. The electronic potential was converted to roll angle (Φ) of the model by LabVIEW with an uncertainty of $\pm 1^\circ$. The acquisition rate is 200Hz and we used MATLAB to calculate the maximum, the minimum, the average and the root-mean-square value from a certain time history of the roll angle Φ.

2.3 Wing Models

We used 10 different models to conduct the experiment. Fig.1 shows the platform of one of them:

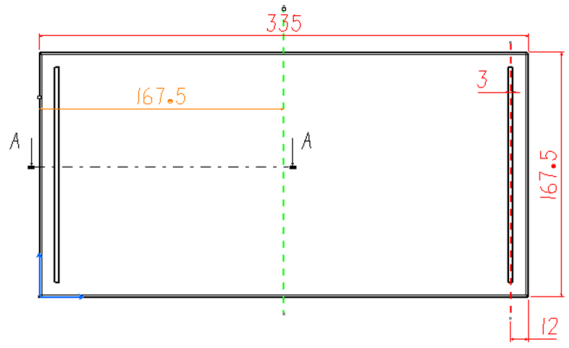

Fig. 1 . Platform of the Model

Each model has a different slot orientation angle β (one without slot as baseline model), defined as Fig.2:

The slots on the 9 slotted models are oriented as: $\beta = 30^\circ$, $\beta = 45^\circ$, $\beta = 60^\circ$, $\beta = 75^\circ$, $\beta = 90^\circ$, $\beta = 105^\circ$, $\beta = 120^\circ$, $\beta = 135^\circ$ and $\beta = 150^\circ$. In the following discussion, they are referred as Model A, Model B, ... , Model I, accordingly. For each of the models, we acquired the roll angle data regarding the angle of attack range of $\alpha = 2^\circ \sim 30^\circ$.

According to the recent work by Pelletier et al.[7], the shape of the model's trailing edge

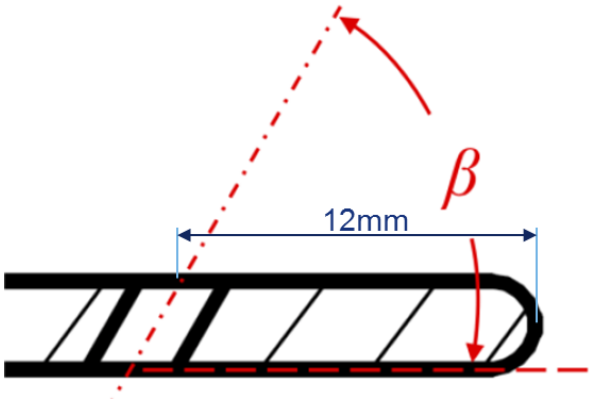

Fig. 2 . Definition of Slot Orientation Angle

would not have a significant effect on the roll performance, and Gresham et al.[8] found that round leading edge could enhance the roll movement. Based on the above fact and to make the result of this paper comparable to the previous works by Hu et al., we rounded the leading edge of the models.

2.4 Near-Surface PIV Measurements

A 2 Dimensional, 2 Component PIV system from MicroVec was used to conduct the near-surface velocity measurements, along with a laser illuminated plane $2mm$ from the model upper surface when $\Phi = 0^\circ$. For dynamic PIV measurement, a synchronizer with an uncertainty within $0.25ns$ was used as a part of the MicroVec PIV system to capture the near suction surface dynamic flow structure.

3 Results and Analysis

3.1 Free-to-Roll Measurements

3.1.1 Roll Response of Baseline Model

The test was conducted at a wing speed of $10m/s$, aligned with the previous studies[9], $Re \approx 1.15 \times 10^5$. The baseline model (without the slots) had similar roll response with the previous works by Gresham et al.[8, 10, 6]: The self-induced roll oscillation occurred at around $\alpha = 13^\circ$, and increased its amplitude slowly as α increased when $13^\circ \leq \alpha \leq 16^\circ$. The amplitude increase acceler-

ated when $16^\circ \leq \alpha \leq 25^\circ$, auto rotation occurred at around $\alpha = 27^\circ$.

3.1.2 Roll Response of Slotted Models

In the conducted experiments, all 9 slotted models showed an ability to attenuate the roll oscillation and the $\beta = 45^\circ$ one (Slot B) stood out. Fig.3 shows the RMS roll angle regarding AoA of the model I and Fig.4 shows the time history of roll angle when $\alpha = 26^\circ$.

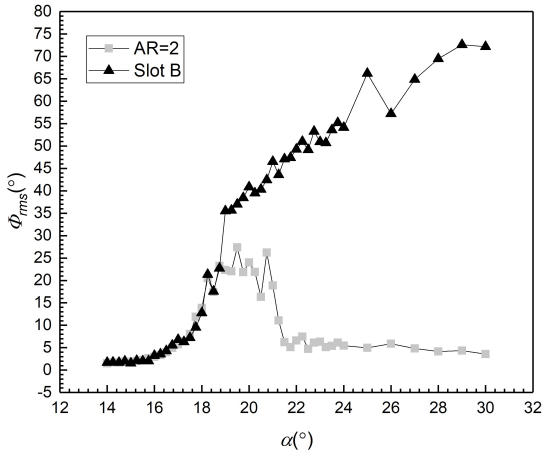

Fig. 3 . RMS Roll Angle, Model B

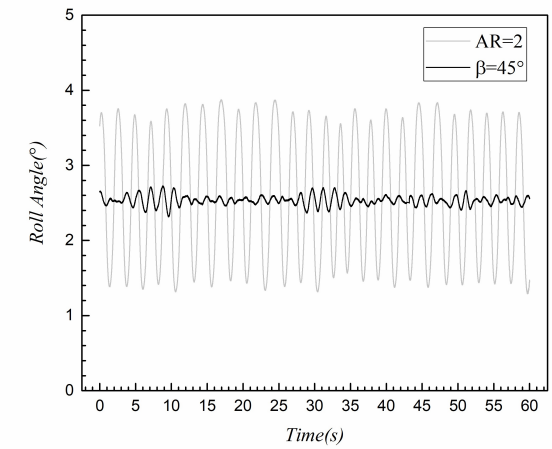

Fig. 4 . Roll Angle Time History, Model B, $\alpha = 26^\circ$

It can be seen from the plots that the roll oscillation was effectively suppressed, especially at high AoA. The occurrence of the wing rock was delayed by about 1°, but the attenuation effect was not significant until AoA reaches around 21°,

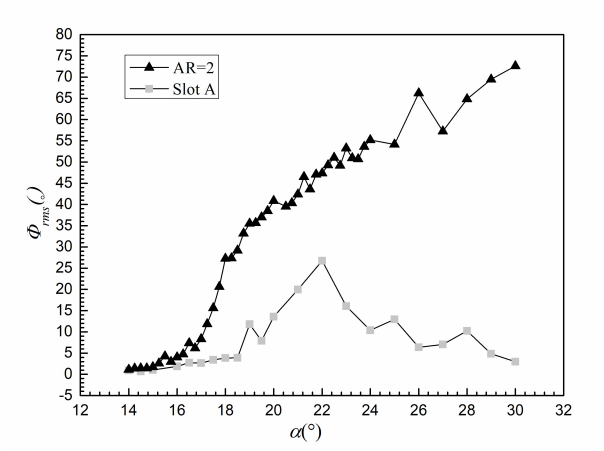

Fig. 5 . RMS Roll Angle, Model A

and the max $\Delta\Phi_{rms} = 14^\circ$ when $18^\circ \leq \alpha \leq 21^\circ$. The roll oscillation $\Delta\Phi_{rms}$ drops to and remains about $3^\circ \sim 4^\circ$ when $\alpha \geq 21^\circ$. The roll angle time history at $\alpha = 26^\circ$ clearly shows the attenuation effect of this configuration at high AoA. It can also be seen from Fig.4 that the roll frequency also decreased at the same time, which would have a positive influence on MAV control. To sum up, the $\beta = 45^\circ$ configuration exhibits the best attenuation effect, up to $\Delta\Phi_{RMS,Max} = 45^\circ$, among all models.

More over, Model A and Model I have also shown decent attenuation effect on wing rock, yet Model H showed an enhancement of the roll oscillation. See the following Fig.5 $\sim$ Fig.7. It can be seen from Fig.5 and Fig.6 that both Model A and Model I have limited attenuating effects comparing to Model B, especially on Model I wing rock occurred earlier (about 0.5°) than the baseline, but on the other hand they both have a similar performance to Model B at high AoA.

Fig.7 shows the RMS roll angle of model H. Unlike any other models tested, this model showed an enhancement to the roll oscillation. Mean while the occurrence of the high amplitude roll oscillation was advanced by about 2°, at around $\alpha = 15^\circ$. The auto rotation happened at $\alpha = 25^\circ$, even earlier than the baseline model. More over, the oscillation builds up in a more dramatic manner comparing to other models. The rest models had relatively similar manners regarding roll response, their RMS roll angle re-

garding AoA plotted in Fig.8.

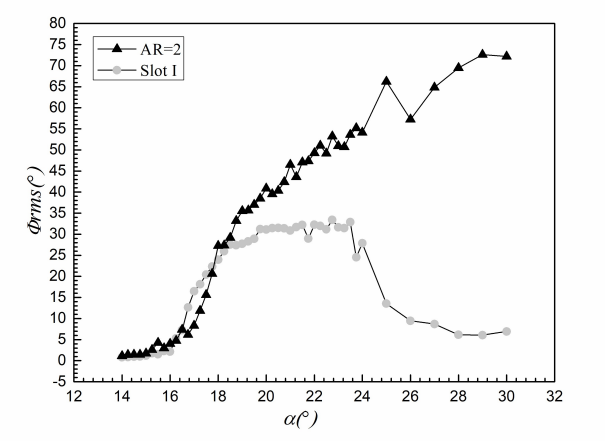

Fig. 6 . RMS Roll Angle, Model I

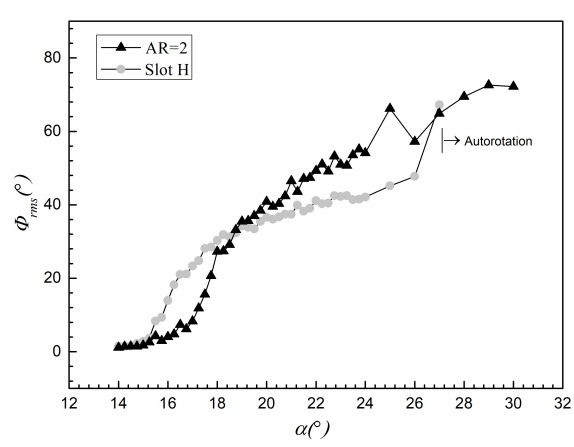

Fig. 7 . RMS Roll Angle, Model H

It can be seen from Fig.8 that the roll response of the rest models in terms of RMS roll angle are quite similar, especially in low AoAs. The attenuating effect diverse at high AoA, yet the differences are not significant.

3.2 Near Surface PIV

From previous studies[6, 8, 10], similar near surface PIV measurements revealed that the roll oscillation results from asymmetric 3D flow structure. The separation bubble prolongs as AoA increases and the wing tip vortex develops further downstream. Meanwhile the interaction becomes greater and leads to asymmetric load on the wing thus oscillation occurs. Fig.9 and Fig.10

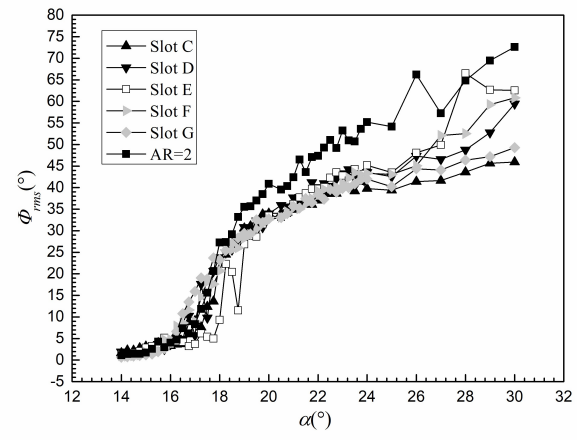

Fig. 8 . RMS Roll Angle, Other Models Tested

demonstrate our near-surface PIV measurements on four of the tested models. Model B and Model I are proven to have the best performance in attenuating roll oscillation and Model D is for the comparing purpose with previous studies[6, 8]. We chose $\alpha = 20^\circ$ as the measuring AoA, as the roll response for each model is most diverse. We choose zero roll angle as the position to indicate the difference of flow patterns of each side on different models.

3.2.1 Stationary Measurements at Zero Roll Angle

Fig.9 shows the near-surface streamlines of the flow on the selected models. At $\alpha = 20^\circ$, there is no sign of the reattachment of the separation bubbles on all four models. Asymmetric flow pattern can be seen on the baseline model, two vortexes can be seen at around $0.7c$. When slot is added, the vortexes are seemingly strengthened by the bleed through the slot for all models, especially for Model B. On the other hand, the strengthened vortexes on two sides are less asymmetric. Is is also noted that the chord-wise position of the core of vortexes on two sides are less on slotted models.

3.2.2 Dynamic Measurements at Zero Roll Angle

Dynamic measurements were conducted in the process of wing oscillation. With the help of the

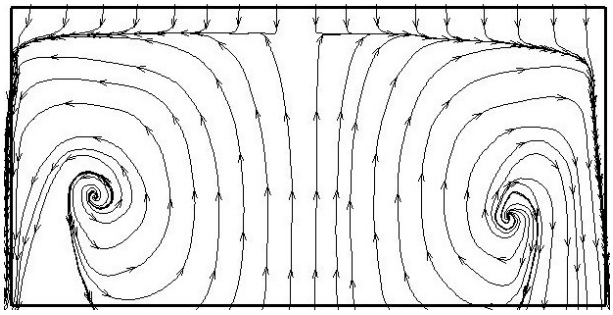

(a) Baseline Model (No Slot)

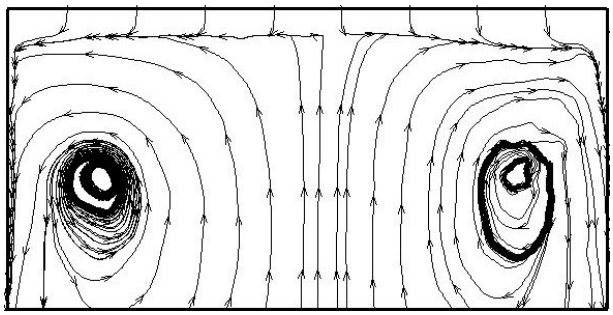

(b) Model B ($\beta = 45°$)

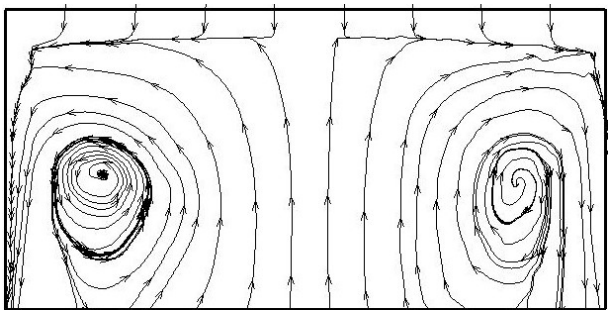

(c) Model D ($\beta = 90°$)

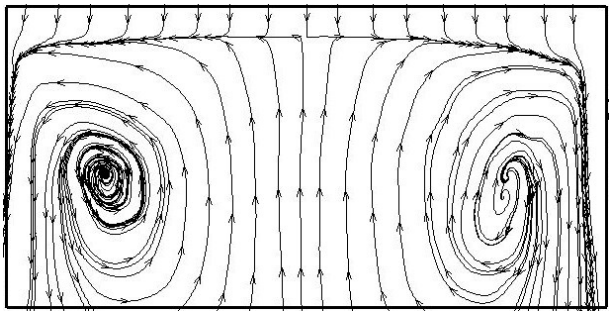

(d) Model I ($\beta = 150°$)

Fig. 9 . Near Surface PIV, Stationary, $\Phi = 0°$, $\alpha = 20°$, $Re = 1.15 \times 10^5$

synchronizer, the camera captures a sequence of 4 pictures when the wing passes $\Phi = 0°$ position (Φ increasing) and calculates the flow field. Fig.10 shows the streamlines from dynamic measurements. It can be seen that the vortex position and strength are very much different from the results from stationary measurements, though the roll angle remains $\Phi = 0°$. Is is also worth noticing that when the wing passes the $\Phi = 0°$ position, the vortex on the right side shall be stronger than the left side. It can also be seen that the left side vortex moves further downstream comparing to the static measurement results. From the cross-flow PIV measurements conducted by Gresham et al.[8], at this position, ($\Phi = 0°$, Φ increasing) the right side vortex is closer to the surface than the left one, and the vortex size on Fig.10 also indicates so. From the streamlines from four models with different oblique slots, it can also seen that as slot angle β increases, the left side vortex is more influenced. Model B and Model I have similarly positioned left vortexes, yet the left side vortex moved further downstream on Model D. One possible explanation would be the bleed through oblique slot can alter the vortex's strength difference on the two sides thus attenuate the oscillation.

The slot orientation angle on Model B and Model I are different yet they achieve similar attenuating effects. Based on the span-wise position of the wing tip vortexes from previous cross-flow PIV measurements[8, 6], possible explanations would be the outward oblique bleed contributes to the vortex already left the surface thus diminish the load difference on the two sides, yet the inward oblique bleed weakens the vortex on the surface, reducing the load difference as well. Yet further cross-flow PIV measurement is required to determine the exact mechanism of this phenomenon and no quantitative conclusion could be drawn at the present.

4 Conclusions

This paper introduced an oblique slot configuration for low aspect ratio (AR=2) rectangular wings to attenuate the self-induced roll oscilla-

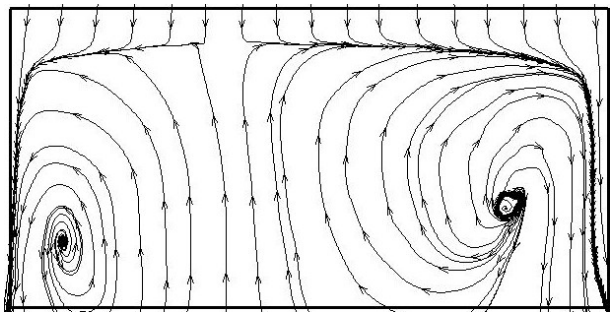

(a) Baseline Model (No Slot)

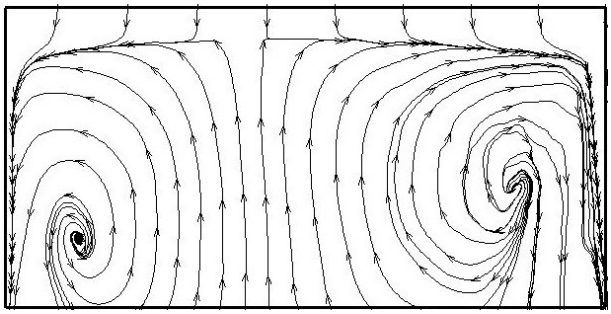

(b) Model B ($\beta = 45°$)

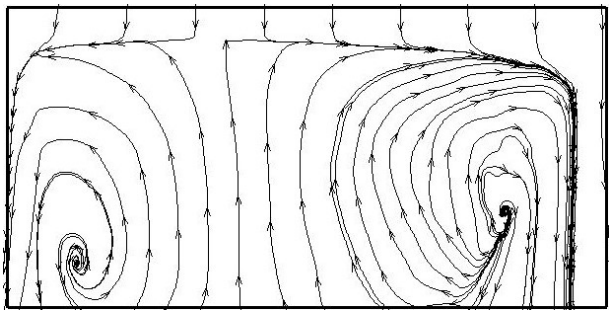

(c) Model D ($\beta = 90°$)

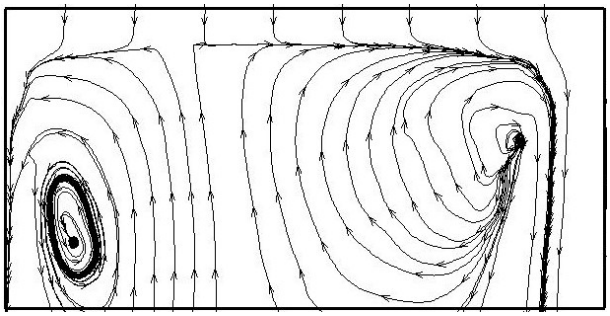

(d) Model I ($\beta = 150°$)

Fig. 10 . Near Surface PIV, Dynamic, $\Phi = 0° +$ (Φ increasing), $\alpha = 20°$, $Re = 1.15 \times 10^5$

tion at low Reynolds numbers. Based on wind tunnel tests conducted on 9 models with different slot orientation, the conclusion can be summarized as follows: 1) The model with slot orientation angle $\beta = 45°$ and $\beta = 150°$ demonstrates the best effect, reducing the RMS roll angle up to $\Delta\Phi \approx 45°$ and $\Delta\Phi \approx 34°$, accordingly; 2) Flow field by PIV measurements indicates that the slotted models have shown more symmetric streamlines, indicating the bleed through oblique slot altering the flow structure to be favorable to load balancing on the two sides of the wing; 3) In some cases ($\beta = 150°$), the added configuration could lead to an increase of the oscillation. Yet no quantitative conclusion could be drawn at the moment and the exact mechanism is still not clear.

5 Contact Author Email Address

If you have any question regarding this paper, please do not heasitate to contact the author by email: tours1994@outlook.com

References

[1] Hutt, G. and East, R. Effects of large oscillation amplitude on axisymmetric vehicle longitudinal static and dynamic stability in hypersonic flow. In *21st Aerospace Sciences Meeting*. American Institute of Aeronautics and Astronautics, 1983.

[2] Levin, D. and Katz, J. Self-induced roll oscillations of low-aspect-ratio rectangular wings. In *17th Atmospheric Flight Mechanics Conference*. American Institute of Aeronautics and Astronautics, 1990.

[3] Arena, A. S. and Nelson, R. C. Experimental investigations on limit cycle wing rock of slender wings. *Journal of Aircraft*, volume 31, no. 5, pages 1148–1155, 1994.

[4] Bakaul, S. R., Wang, Y., and Guangxing, W. Effect of Vertical Strakes on Suppression of Wing Rock in Slender Delta Wing. In *53rd AIAA Aerospace Sciences Meeting*. American Institute of Aeronautics and Astronautics, 2015.

[5] Hu, T., Wang, Z., and Gursul, I. Attenuation of Self-Excited Roll Oscillations of Low-Aspect-Ratio Wings by Using Acoustic Forc-

ing. *AIAA Journal*, volume 52, no. 4, pages 843–854, 2014.

[6] Hu, T., Wang, Z., and Gursul, I. Passive Control of Self-Induced Roll Oscillations Using Bleed. In *52nd Aerospace Sciences Meeting*. American Institute of Aeronautics and Astronautics, 2014.

[7] Pelletier, A. and Mueller, T. J. Low Reynolds Number Aerodynamics of Low-Aspect-Ratio, Thin/Flat/Cambered-Plate Wings. *Journal of Aircraft*, volume 37, no. 5, pages 825–832, 2012.

[8] Gresham, N., Wang, Z., and Gursul, I. Aerodynamics of Free-to-Roll Low Aspect Ratio Wings. In *47th AIAA Aerospace Sciences Meeting including The New Horizons Forum and Aerospace Exposition*. American Institute of Aeronautics and Astronautics, 2009.

[9] Hu, T., Wang, Z., and Gursul, I. Passive control of roll oscillations of low-aspect-ratio wings using bleed. *Experiments in Fluids*, volume 55, no. 6, pages 1–16, 2014.

[10] Hu, T., Wang, Z., and Gursul, I. Control of Self-Excited Roll Oscillations of Low-Aspect-Ratio Wings Using Acoustic Excitation. In *49th AIAA Aerospace Sciences Meeting including the New Horizons Forum and Aerospace Exposition*. American Institute of Aeronautics and Astronautics, 2011.

Copyright Statement